Nonquenchable Chemical Order−Disorder Phase Transition in Yttrium Oxyfluoride

Igor Levin,*[a] Qing Z. Huang,[a] Lawrence P. Cook,[a] and Winnie Wong-Ng[a]

Keywords: Phase transitions / Yttrium / X-ray diffraction / Order−disorder transitions

A chemical order–disorder polymorphic phase transition in yttrium oxyfluoride (YOF) was studied in situ by X-ray and neutron powder diffraction. The high-temperature form of YOF crystallizes with a cubic $Fm\bar{3}m$ fluorite structure in which the O and F atoms are disordered among the tetrahedrally coordinated sites. The low-temperature form of YOF exhibits rhombohedral $R\bar{3}m$ symmetry and evolves from the high-temperature form by the phase transition associated with the ordering of the O and F atoms. The transition occurs around 560 °C. The superstructure contains layers of $[OY_4]$ and $[FY_4]$ tetrahedra alternating along the *c*-axis of the trigonal cell (parallel to the <111> direction of the parent cubic structure). The ordering of the O and F atoms is accompanied by the significant displacements of the Y, O, and F atoms from their ideal positions in the cubic phase. Bond valence sum calculations indicate considerable bond strain for both O and F in the cubic structure; the strain is relieved in the ordered low-temperature phase. The order–disorder transition in YOF is completely reversible and exhibits fast nonquenchable kinetics.

Introduction

Phase equilibria in the Ba−Cu−Y−F−O system have become the subject of intensive investigation after the BaF_2−Cu−Y precursor films, deposited on RABiTS and annealed in water vapor, demonstrated the potential for producing high quality $Ba_2YCu_3O_{6+x}$ (Y-213) superconductor tapes.[1] One of the critical questions in studies of phase equilibria in this system concerns the existence of the transient fluorine-containing low-temperature melts, which could control formation of the Y-213 phase. Recent systematic studies of melting temperatures in the $BaF_2-YF_3-Y_2O_3-CuO_x$ subsystem using differential thermal analysis (DTA) showed a peak at T = 560 °C that could be attributed to such a transient melt.[2] However, subsequent analyses of these samples using variable-temperature X-ray powder diffraction demonstrated that this DTA event is associated with a nonquenchable phase transition in the stoichiometric yttrium oxyfluoride.[2] The crystal structure of YOF has been studied previously.[3,4] Zachariasen[3] reported both rhombohedral and tetragonal room-temperature forms of YOF. The tetragonal form is stabilized by the excess fluorine and occurs for the compositions YO_nF_{3-2n} with $0.7 < n < 1.0$, whereas the rhombohedral structure is stable for the stoichiometric composition with n = 1. Both structures have been described as derivatives of the cubic fluorite archetype with the ordering of oxygen and fluorine atoms into distinct tetrahedrally coordinated sites. Later X-ray diffraction studies by Bevan and Mann[4] confirmed the rhombohedral structure of stoichiometric YOF with the space group $R\bar{3}m$ (a = 3.797 Å, c = 18.89 Å). Zachariasen[2] has alluded to the potential existence of the disordered high-temperature cubic fluorite phase; however, all attempts to quench the cubic form were unsuccessful. Later studies[3−7] confirmed the existence of the rhombohedral ⇄ cubic phase transition in YOF at 560−570 °C, but provided few details on the evolution of structural parameters upon this phase change. In the present contribution, we report a detailed study of such nonquenchable order−disorder phase transition in stoichiometric YOF as analyzed in situ by variable-temperature X-ray and neutron powder diffraction.

[a] Materials Science and Engineering Laboratory, National Institute of Standards and Technology, Gaithersburg, MD 20899, USA

Results and Discussion

The room temperature X-ray powder diffraction patterns of YOF, both slowly cooled and quenched from 600 °C, were completely indexable according to the rhombohedral (R) unit cell with lattice parameters a_R = 3.800(5) Å and c_R = 18.863(9) Å. In addition to the major YOF phase, the sample contained small amounts of Y_2O_3. As the Y_2O_3 reflections do not overlap with those of YOF, they do not affect the refinement of the YOF structure and were excluded from the analysis. In situ studies of the YOF sample with high-temperature X-ray diffraction revealed a reversible phase transformation to a cubic (C) structure as inferred from the disappearance of the rhombohedral reflec-

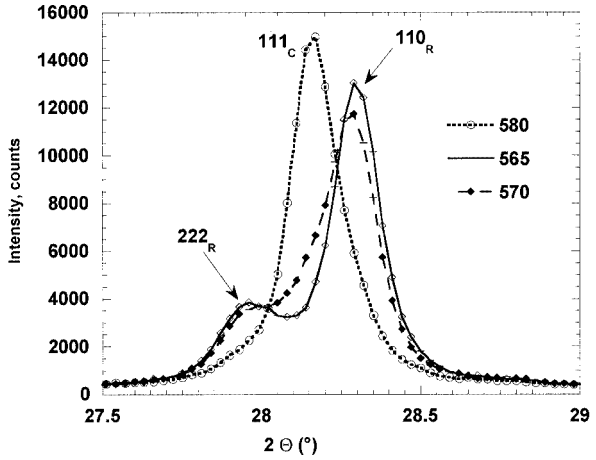

Figure 1. Evolution of the $222_R/110_R$ and 111_c reflections upon heating/cooling across the rhombohedral ⇄ cubic transition during in situ X-ray powder diffraction measurements

tion splitting (Figure 1). The transition occurred at $T_0 \approx$ 575 °C, which is in reasonable agreement with T_0 = 565 °C deduced from the DTA measurements (Figure 2).

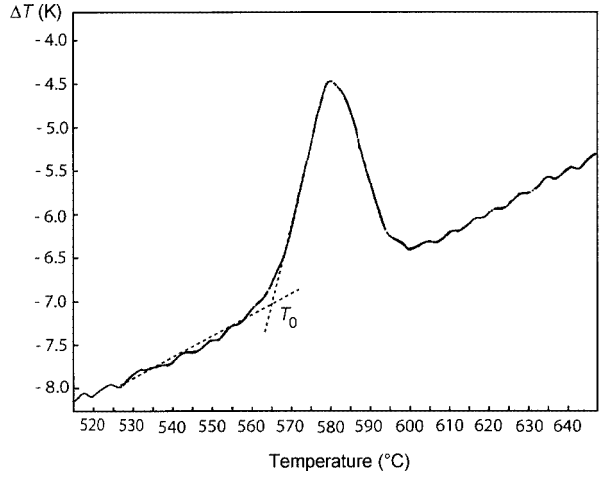

Figure 2. DTA plot for YOF; the transition temperature was determined from the extrapolated intersection of the baseline with the linear portion of the rising peak

Structural refinements using neutron powder diffraction data (Table 1, Figure 3, a) and the initial atomic positional parameters from ref.[4] confirmed that the low-temperature

Table 1. Refined structural parameters for the rhombohedral and cubic YOF polymorphs

Atom	x	y	z	$U_{iso}\times100$ Å^2
T = 514 °C K, $R\bar{3}m$, a = 3.8205(2) Å, c = 19.019(1) Å				
Y	0	0	0.2418(1)	1.40(4)
F	0	0	0.3698(1)	2.61(7)
O	0	0	0.1211(1)	1.89(6)
T = 613 °C, $Fm\bar{3}m$, a = 5.4527(2) Å				
Y	0	0	0	2.99(4)
O/F	1/4	1/4	1/4	3.51(4)

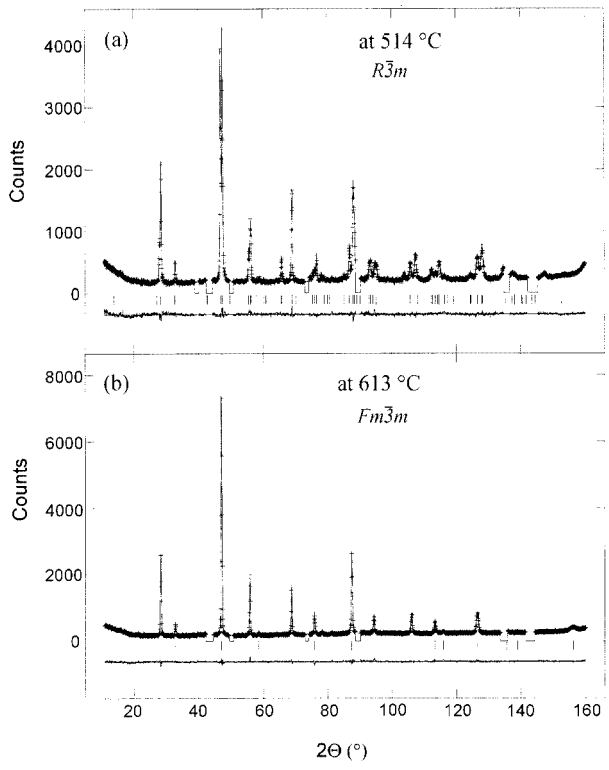

Figure 3. (Upper) Experimental (crosses) and calculated (line) neutron powder diffraction profiles of YOF acquired at a) 514 °C (rhombohedral phase), and b) 613 °C (cubic phase); regions containing reflections of the impurity phase were excluded from the fit; (lower) residual; the fitting reliability parameters are R_{wp} = 6.22%, χ = 1.18 for T = 514 °C, and R_{wp} = 6.32, χ = 1.20 for T = 613 °C

YOF polymorph crystallizes with a rhombohedral $R\bar{3}m$ superstructure. The superstructure features layers of [FY_4] and [OY_4] tetrahedra alternating along the c_R-axis (Figure 4). The atomic positional and displacement parameters refined for T = 514 °C are summarized in Table 2. In the rhombohedral structure, all three species, Y, O, and F, exhibit appreciable displacements (v_Y = 0.0082c_R, v_F =

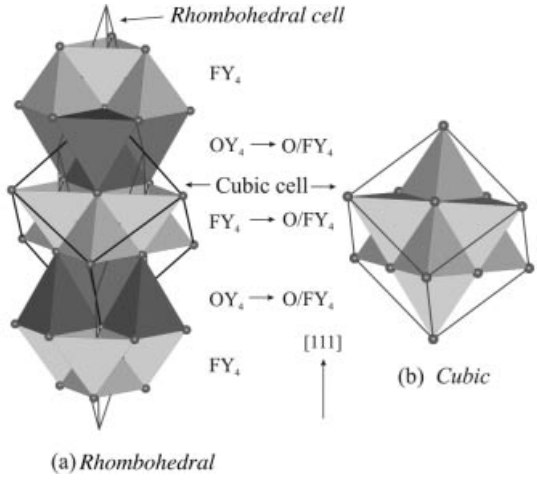

Figure 4. Schematic representation of the refined YOF rhombohedral (left) and cubic fluorite (right) structures

$0.0052c_R$, $v_O = 0.0039c_R$) from the ideal positions in the cubic fluorite; the displacements occur along the *c*-axis, which is parallel to the $<111>_c$ direction of the cubic fluorite. The resulting Y−F bond distances (2.435 Å and 2.4412 Å) are significantly longer than the corresponding Y−O distances (2.297 Å and 2.2763 Å). Refinements of anisotropic temperature parameters did not reveal any significant anisotropy of displacements and produced little effect on the quality of the fit; therefore, in the final refinement run, the temperature parameters were assumed to be isotropic. As the site occupancies refined for the O and F positions were within the estimated standard uncertainties (2%) from the ideal values of unity, both positions were assumed to be fully occupied. Both $[FY_4]$ and $[OY_4]$ tetrahedra are appreciably distorted (Figure 5) as seen from comparison of both Y−F−Y (115.4°/103.0°) and O−Y−O (114.1°/104.3°) angles with a value of 109.47° in a perfect tetrahedron.

Table 2. Selected bond distances, and calculated BVS values for the YOF polymorphs

F−Y (Å)	O−Y (Å)
Rhombohedral (T = 514 °C)	
2.435(4)	2.297(4)
2.4412(9) ×3	2.2763(5)
BVS = 0.94 v.u.	*BVS* = 1.94 v.u .
Cubic (T = 613 °C)	
2.3611(1)	2.3611(10)
BVS = 1.16 v.u.	*BVS* = 1.57 v.u.
Average *BVS* = 1.37 v.u.	

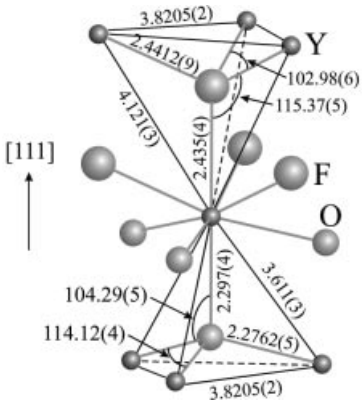

Figure 5. Coordination environment of the Y atoms in the YOF rhombohedral structure at 514 °C; selected bond distances and angles are indicated

Heating the YOF sample in situ during the neutron diffraction measurements caused a reversible phase transition to the cubic structure (Figure 6); the transition temperature T = 520 °C in the neutron experiments is lower than that determined with both DTA and X-ray diffraction. The lower value of T_0 from the neutron measurements was attributed to the temperature gradient in the furnace (up to 10 °C) combined with slow conduction of heat from the vacuum of the furnace through the container wall to the YOF powder. The neutron diffraction patterns recorded at T = 500 °C and T = 540 °C (on the thermocouple) contained single rhombohedral and cubic phases, respectively. In contrast, the neutron diffraction pattern recorded at 520 °C contained a two-phase mixture. Given the nonquenchable kinetics of the rhombohedral ⇄ cubic phase transition, the coexistence of these two phases at T = 520 °C for a prolonged time was attributed to thermal gradients across the relatively large neutron sample. The temperature dependence of the lattice parameters refined for the YOF polymorphs is summarized in Figure 7. The rhombohedral ⇄ cubic transition appears to be a first-order transition and is accompanied by a volume change of about 0.6%.

A structural model based on the ideal cubic fluorite structure (space group $Fm\bar{3}m$) with a disordered mixture of F and O atoms on the fourfold coordinated sites (Table 2) provided a satisfactory fit to the experimental data at T =

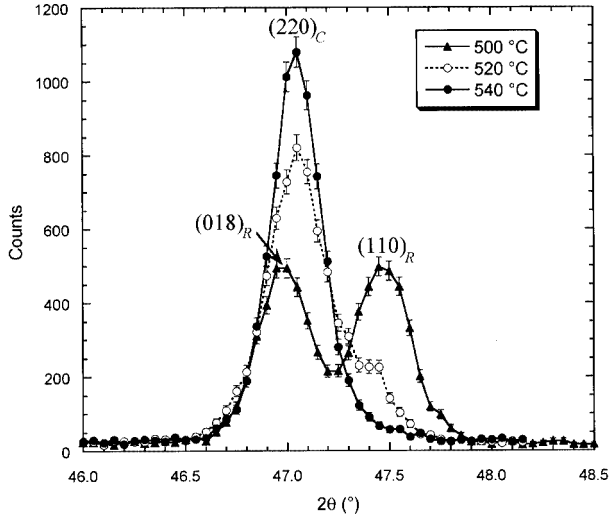

Figure 6. Evolution of the $110_R/108_R$ and 220_c neutron reflections upon heating/cooling across the rhombohedral ⇄ cubic transition; at T = 520 °C (on the thermocouple) a two-phase mixture is observed, presumably due to the thermal gradients in the sample

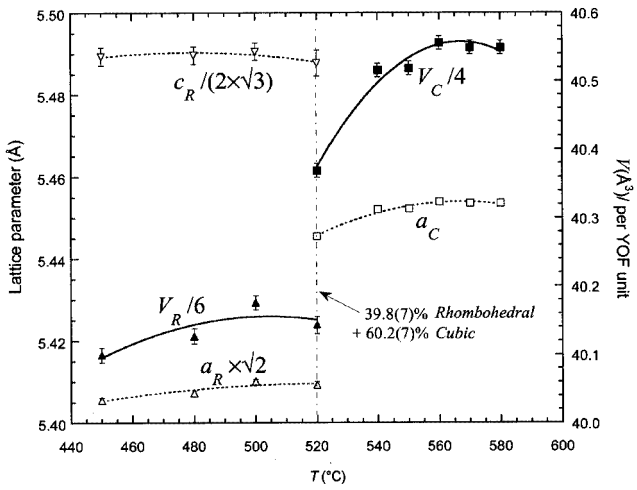

Figure 7. Temperature dependence of the lattice parameters for the rhombohedral and cubic phase; a significant volume change upon the rhombohedral ⇄ cubic transition is observed

613 °C (see b in Figure 3). The symmetries of the high-temperature cubic and low-temperature rhombohedral phases obey a group−subgroup relation.

Bond valence sum (BVS) calculations for this cubic structure indicate strong under- and over-bonding for the O and F atoms, respectively, whereas the bond requirements for Y are closely satisfied. Such strong deviations from the ideal BVS values suggest the existence of *local* atomic displacements in the cubic structure aimed to accommodate the bonding requirements of the O and F atoms. Indeed, values of the temperature/displacement parameters for the Y and O atoms increased discontinuously upon transition to the cubic phase (Figure 8), which can be attributed to disordered local displacements of these atoms from their ideal positions in the cubic structure. Interestingly, temperature parameters for the over-bonded F atoms displayed no evidence for such local displacements. In contrast to the cubic phase, the low-temperature rhombohedral phase features nearly ideal BVS values for both O and F atoms. The BVS analyses suggest that simultaneous satisfaction of the bonding requirements for the O and F atoms, which cannot be achieved in the ideal cubic fluorite arrangement, provides a driving force for the O/F ordering and the associated ion displacements. Fast nonquenchable kinetics for the O/F order−disorder transition in YOF can be attributed to the high anion mobility often observed in fluorite-based ion conductors.

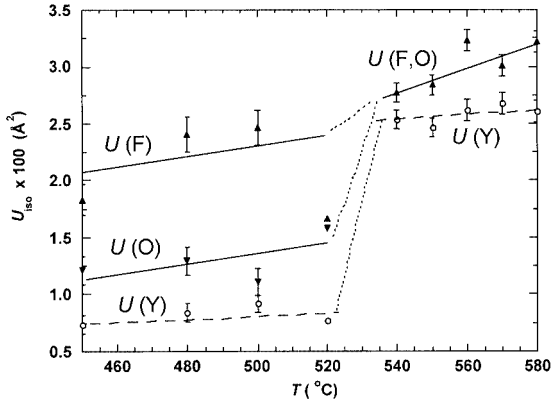

Figure 8. Temperature dependence of the isotropic temperature/displacement parameters, U_{iso}, for the Y, O, and F atoms in the YOF polymorphs; the U_{iso} parameters for both Y and O, but not F, exhibit a discontinuous increase upon the rhombohedral ⇄ cubic transition; such an abrupt increase in the magnitude of U_{iso} suggests the presence of local disordered displacements of both Y and O atoms in the cubic phase

Conclusions

YOF crystallizes with two polymorphs separated by the F/O order−disorder phase transition at T = 560 °C. The high-temperature form features a cubic $Fm\bar{3}m$ fluorite structure − the O and F atoms are disordered on the tetrahedrally coordinated sites. The ordering of F and O atoms upon transition to the low-temperature phase yields rhombohedral $R\bar{3}m$ symmetry and the lattice parameters $a_R \approx a_C/\nu 2$, $c_R \approx 2a_C\nu 3$. This fluorite-based superstructure contains layers of $[OY_4]$ and $[FY_4]$ tetrahedra alternating along the *c*-axis of the trigonal cell (parallel to the <111> direction of the parent cubic structure). The ordering of the O and F atoms is accompanied by the displacements of the Y, O, and F atoms from their ideal positions in the cubic phase. Bond valence sum calculations indicate considerable bond strain for both O and F in the cubic structure. The refinements suggest significant local displacements for the O and Y atoms (but not F), which are likely aimed to satisfy the bonding requirements of the anions. The bond strain about both O and F is relieved in the ordered low-temperature phase. The order−disorder transition in YOF is reversible and exhibits fast nonquenchable kinetics.

Experimental Section

Polycrystalline samples of YOF were prepared using powders of Y_2O_3 (Alfa Industries, lot # 093080, 99.999% purity, metals basis) and anhydrous YF_3 packed under Ar (Alfa Aesar lot # D10 K11, 99.9% purity, metals basis). Prior to use, the Y_2O_3 was preheated at 600 °C for 1 h to remove moisture. A 5-g mixture of Y_2O_3 and YF_3 in equimolar proportion was weighed in an Ar-filled glovebox with a continuously recirculating purifier, which removed contaminants to <1 ppm by volume. The powder mixture was transferred to a thermoanalyzer and annealed overnight at 500 °C in flowing Ar; the powder was contained in a platinum-lined crucible to prevent any reaction of YF_3 with the ceramic crucible. This procedure was repeated with intermediate grindings five times. The total mass lost during synthesis was 0.4 wt.-%.

Simultaneous differential thermal analysis/thermogravimetric analysis (DTA/TGA) experiments were completed in a Mettler TA1 thermoanalyzer outfitted with Anatech digital control and data acquisition electronics. DTA crucibles were fabricated from high purity Pt tubing, and experiments were conducted at a ramp rate of 10 °C/min. Phase-transition onset temperatures during heating were determined from extrapolated intersection of the baseline with the linear portion of the rising peak. The DTA apparatus was calibrated against the α→b quartz transition (571 °C) and the NaCl melting point (801 °C); DTA temperatures were estimated to have < ±3 °C standard uncertainty.

High-temperature X-ray diffraction (HTXRD) measurements were conducted in a Siemens 5000 θ−θ diffractometer equipped with a high-temperature furnace and a position sensitive detector. Cu-K_α radiation was used. The samples were prepared by applying a thin layer of powder (finely ground as an ethanol slurry) to a Pt heating band. The X-ray diffraction experiments were conducted under He gas flow.

Neutron powder diffraction data for Rietveld analysis were collected on the BT1 diffractometer at the Center for Neutron Research at the National Institute of Standards and Technology, using a Cu(311) monochromator with a wavelength of 1.5402(2) Å, and an array of 32 He-3 detectors at 5° intervals. Collimation of 15′, 20′, and 7′ arc were used before and after the monochromator, and after the sample, respectively. The YOF sample was held in a vanadium cylindrical sample container and heated in a furnace under vacuum. The data were collected over the 2θ range 3−168 ° at 11 temperatures between 450 °C and 613 °C. The GSAS package[8] was used for Rietveld structural refinements.

[1] R. Feenstra, T. B. Lindemer, J. D. Budai, M. D. Galloway, *J. Appl. Phys.* **1991**, *69*, 6569.
[2] W. Wong-Ng, L. P. Cook, I. Levin, M. Vaudin, J. Suh, and R. Feenstra, *J. Mater. Res.,* to be submitted.
[3] W. H. Zachariasen, *Acta Crystallogr.* **1957**, *4*, 231−236.
[4] A. W. Mann, D. J. M. Bevan, *Acta Crystallogr., Sect. B* **1970**, *26*, 2129−2131.
[5] J. H. Miller, T. Petzel, *J. Alloys and Comp.* **1995**, *224*, 18−21.
[6] T. Petzel, V. Marx, B. Hormann, *J. Alloys and Comp.* **1993**, *200*, 27−31.
[7] K. Niihara, S. Yajima, *Bull. Chem. Soc. Jpn.* **1972**, *44 (3)*, 20−23.
[8] A. C. Larson and R. B. Von Dreele, "*General Structure Analysis System*", Los Alamos National Laboratory Report, LAUR 86−748, **1994**.

Received April 14, 2004
Early View Article
Published Online November 10, 2004

